Hyperactivation of nuclear factor of activated T cells 1 (NFAT1) in T cells attenuates severity of murine autoimmune encephalomyelitis

Srimoyee Ghosh[a], Sergei B. Koralov[a], Irena Stevanovic[a], Mark S. Sundrud[a], Yoshiteru Sasaki[a,b], Klaus Rajewsky[a], Anjana Rao[a,1], and Martin R. Müller[a,c,1]

[a]Department of Pathology, Harvard Medical School and Immune Disease Institute and Program in Cellular and Molecular Medicine, Children's Hospital, Boston, MA 02115; [b]Laboratory for Stem Cell Biology, RIKEN Center for Developmental Biology, Kobe 650-0047, Japan; and [c]Department of Hematology, Oncology, and Immunology, Universitätsklinikum Tübingen, Medizinische Klinik und Poliklinik, 72076 Tübingen, Germany

Contributed by Anjana Rao, June 30, 2010 (sent for review April 17, 2010)

Nuclear factor of activated T cells (NFAT) proteins are a group of Ca^{2+}-regulated transcription factors residing in the cytoplasm of resting cells. Dephosphorylation by calcineurin results in nuclear translocation of NFAT and subsequent expression of target genes; rephosphorylation by kinases, including casein kinase 1 (CK1), restores NFAT to its latent state in the cytoplasm. We engineered a hyperactivable version of NFAT1 with increased affinity for calcineurin and decreased affinity for casein kinase 1. Mice expressing hyperactivable NFAT1 in their T-cell compartment exhibited a dramatically increased frequency of both IL-17– and IL-10–producing cells after differentiation under Th17 conditions—this was associated with direct binding of NFAT1 to distal regulatory regions of *Il-17* and *Il-10* gene loci in Th17 cells. Despite higher IL-17 production in culture, the mice were significantly less prone to myelin oligodendrocyte glycoprotein peptide-induced experimental autoimmune encephalomyelitis than controls, correlating with increased production of the immunomodulatory cytokine IL-10 and enhanced accumulation of regulatory T cells within the CNS. Thus, NFAT hyperactivation paradoxically leads to decreased susceptibility to experimental autoimmune encephalomyelitis, supporting previous observations linking defects in Ca^{2+}/NFAT signaling to lymphoproliferation and autoimmune disease.

autoimmunity | experimental autoimmune encephalomyelitis | IL-10 | Treg

Nuclear factor of activated T cells (NFAT) proteins regulate the early stages of T-cell activation—they are particularly critical in guiding the differentiation of naïve CD4 T cells into distinct effector T-cell subsets, controlling IFNγ expression by Th1 cells and IL-4, IL-5, and IL-13 expression by Th2 cells (1, 2). Recent studies have implicated NFAT in the expression of IL-17 and IL-21, signature cytokines of the Th17 effector lineage (3): the IL-21 promoter is transactivated by NFAT (4), and the Tec family tyrosine kinase, inducible T-cell kinase (Itk), is thought to couple T-cell receptor (TCR) signaling to IL-17 expression through NFAT2 (5). NFAT also controls the activity of regulatory T cells (Tregs) through modulating levels of Foxp3 and cooperates with the latter to regulate expression of several characteristic genes in Tregs; NFAT-Foxp3 cooperation is essential for Treg function in a mouse model of autoimmune diabetes (6–8).

NFAT nuclear translocation occurs in response to dephosphorylation by the Ca^{2+}-activated phosphatase calcineurin and is countered by NFAT kinases such as CK1, GSK3, and DYRK (1, 9). To probe the biological functions of NFAT, we designed a hyperactivable mutant of NFAT1 (10), the predominant family member present in naïve T cells (11)—the calcineurin docking site (SPRIEIT) was substituted with a higher affinity version (HPVIVIT), and conversely, the CK1 docking site (FSILF) was substituted with a lower affinity version (ASILA) (Fig. S1*A*) (12, 13). Expectedly, ASILA-VIVIT-NFAT1 (AV-NFAT1) was hyperresponsive to Ca^{2+} signals compared with wild-type NFAT1 (10); unlike constitutively active (CA)-NFAT1 (11), its transcriptional activity was completely blocked by the calcineurin inhibitor cyclosporin A (CsA), indicating that it retains its dependence on Ca^{2+}/calcineurin signals for activation (10).

To analyze how the pleiotropic effects of NFAT on T-cell lineage commitment would balance out in vivo, we generated transgenic mice that conditionally express AV-NFAT1 from the *Rosa26* (R26) locus in T cells (AVT mice) (10). We show that naïve T cells from these mice exhibit a significantly increased frequency of both IL-17– and IL-10–producing cells on differentiation under Th17 conditions; this correlated with the ability of NFAT1 to bind directly to regulatory regions of the *Il17* and *Il10* gene loci in T cells undergoing Th17 differentiation. AVT mice were less susceptible than control animals to the development of myelin oligodendrocyte glycoprotein peptide (MOG)-induced experimental autoimmune encephalomyelitis (EAE). Despite lower overall numbers of $Foxp3^+$ cells in spleen and lymph nodes of AVT mice, Tregs expressing AV-NFAT1 showed enhanced suppressive activity compared with control Tregs in coculture assays and accumulated in increased amounts in the CNS of AVT mice after EAE induction. Taken together, our data emphasize the diverse and often opposing effects of NFAT signaling on immune function in vivo and show that gain of NFAT function can be associated, perhaps paradoxically, with amelioration of autoimmune disease.

Results

$R26^{AV\text{-}NFAT1}/R26^{AV\text{-}NFAT1}$ and $R26^{AV\text{-}NFAT1}/R26^{+}$ mice, homozygous and heterozygous, respectively, for the AV-NFAT1-IRES-GFP transgene in the R26 locus were crossed to CD4-Cre mice that turn on Cre recombinase selectively in the T-cell lineage at the double-positive stage of thymocyte development. The resulting homozygous $R26^{AV\text{-}NFAT1}/R26^{AV\text{-}NFAT1}$ CD4-Cre and heterozygous $R26^{AV\text{-}NFAT1}/R26^{+}$ CD4-Cre mice, which express AV-NFAT1 and GFP in CD4 and CD8 T cells (Fig. S1*B*), were phenotypically indistinguishable and are referred to as AVT mice. The AV-NFAT1–expressing T cells and Treg cells in AVT mice are designated AV T cells and AV Tregs, respectively.

Th1 Bias, Increased Th17 Differentiation, and Complex Treg Properties in AVT Mice. AVT mice were born at normal Mendelian ratios with no overt signs of pathology and no major perturbations in most lymphoid compartments (Fig. S2 *A* and *B*). The frequency of effector T cells with an activated CD4 $CD44^{hi}CD62L^{lo}$ surface phenotype was significantly reduced in AVT mice compared with wild type (WT), corroborating the previously observed increase of this population in $NFAT1^{-/-}$ animals (Fig. S2*C*) (14, 15);

Author contributions: S.G., A.R., and M.R.M. designed research; S.G., S.B.K., I.S. and M.S.S. performed research; Y.S. and K.R. contributed new reagents/analytic tools; and S.G., A.R., and M.R.M. wrote the paper.

The authors declare no conflict of interest.

[1]To whom correspondence may be addressed. E-mail: Martin.Mueller@med.uni-tuebingen.de or arao@idi.harvard.edu.

This article contains supporting information online at www.pnas.org/lookup/suppl/doi:10.1073/pnas.1009193107/-/DCSupplemental.

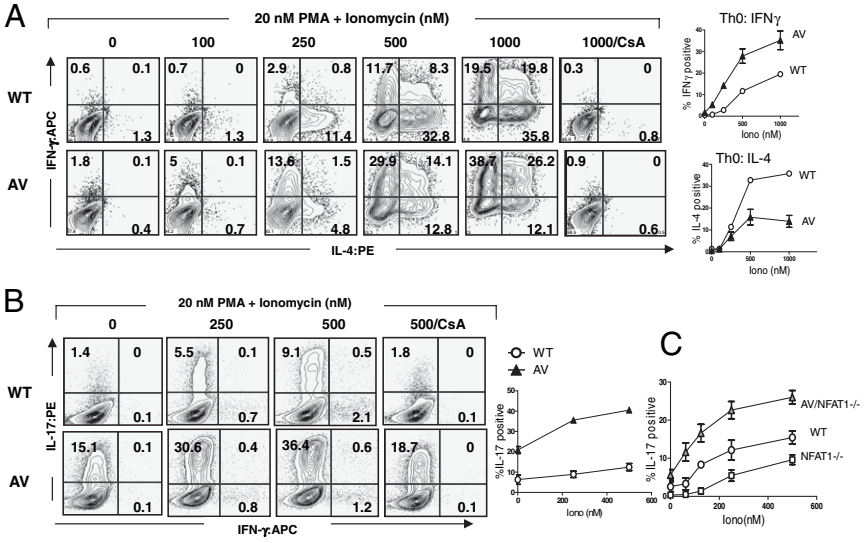

Fig. 1. Cytokine production by cultured T cells from WT and AVT mice. (*A*) CD4 T cells from AVT and WT mice were differentiated under non-polarizing (Th0) conditions. Cells were allowed to rest and restimulated on day 5 with 20 nM PMA and the indicated concentrations of ionomycin. (*B*) Naïve CD4 T cells from WT and AVT mice were differentiated under Th17 conditions and restimulated on day 4 with 20 nM PMA and indicated concentrations of ionomycin. (*C*) Naïve CD4 T cells from WT, NFAT1-/- and AVT NFAT1-/- mice were differentiated under Th17 conditions and restimulated as in *B*. Data are representative of at least two independent experiments.

absolute numbers were also slightly decreased, but the decrease did not approach statistical significance (Fig. S2*C*).

On activation under nonpolarizing (Th0) conditions, CD4 T cells from AVT mice exhibited a marked Th1 bias, yielding higher percentages of IFNγ-producing cells and lower percentages of IL-4–producing cells compared with WT (Fig. 1). The Th1 bias of AV T cells was maintained on differentiation under Th2 conditions (Fig. S3*A*), consistent with the previously noted Th2 bias of NFAT1$^{-/-}$ mice (14, 15). In contrast, differentiation under Th1 conditions yielded equivalent percentages of IFNγ-producing CD4 T cells from WT and AVT mice (Fig. S3*A*). On in vitro activation, CD8 T cells from AVT mice also produced higher frequencies of IFNγ- and IL-2–positive cells relative to WT (Fig. S3*B*), again consistent with the known properties of NFAT1$^{-/-}$ CD8 T cells (16).

Naïve CD4 T cells from AVT mice showed an increased proclivity to Th17 differentiation in vitro, yielding 2- to 4-fold higher frequencies of IL-17–producing cells compared with WT (Fig. 1*B*). Increased IL-17 production was also observed on retroviral transduction of primary CD4 T cells from WT C57BL/6 mice with CA-NFAT1 under Th17-inducing conditions (Fig. S4*A*). Notably, AV T cells produced increased amounts of IL-17 compared with WT T cells in response to phorbol myristate acetate (PMA) stimulation alone (Fig. 1*B Left*), and IL-17 production by AV T cells in response to both PMA and ionomycin was only partially inhibited by CsA (Fig. 1*B Right*), suggesting involvement of a Ca^{2+}-independent arm of the TCR signaling pathway that is activated downstream of AV-NFAT1. Conversely, naïve CD4 T cells from NFAT1$^{-/-}$ animals produced decreased levels of IL-17 relative to WT (Fig. 1*C*), consistent with the absolute requirement for TCR signaling and proposed central role for NFAT in Th17 differentiation (5, 17).

On culture under Th17 conditions, AV T cells up-regulated retinoic acid receptor related orphan receptor (ROR)γt mRNA to a greater extent than WT at a relatively early time point (8 h postactivation), although they did not exhibit the substantial increase in transcript levels observed in WT T cells by 24 h postactivation (Fig. S4*B*). Similarly, AV T cells produced increased amounts of interferon regulatory factor (IRF)4 mRNA at early times after stimulation, but the levels of IRF4 transcripts decayed more quickly than in WT (Fig. S4*C*). By 48 h, however, AV and WT T cells had roughly equivalent mRNA levels of both RORγt and IRF4. Early Th17 differentiation is also associated with transient expression of Foxp3, which antagonizes RORγt function—Foxp3 levels decline with gradual progression of the Th17 program (18). AV T cells exhibited increased and faster down-regulation of Foxp3 transcripts compared with WT T cells (Fig. S4*D*). Early induction of Th17 transcriptional regulators in AV T cells, coupled with enhanced down-modulation of Foxp3 (particularly at the intermediate 24-h time point where RORγt and IFR4 transcript levels are lower in AV T cells), could confer on them an early selective advantage towards Th17 differentiation. Additionally, IL-21 levels were increased in AVT mice compared with WT (Fig. S4*E*)—this could be because of the early spike in IRF4 levels in AV T cells, direct binding of NFAT to the *Il21* locus, or both (4, 19). Given its role as an important Th17 lineage-specification factor (20), increased levels of IL-21 could at least partly explain the enhanced propensity of AV CD4 T cells for Th17 differentiation.

The Treg phenotype in AVT mice was complex and notably dichotomous. There were fewer Tregs in AVT mice at steady state compared with WT (Fig. 2 *A* and *B*), but their suppressive capacity was superior to that of WT Tregs, as assessed by the ability to inhibit T-cell proliferation in vitro (Fig. 2 *C* and *D*, and Fig. S5). Additionally, naïve CD4 T cells from AVT mice generated significantly higher proportions of Foxp3$^+$ T cells (iTregs) on activation in vitro in the presence of TGFβ (Fig. 2*E*).

AVT Mice Are Less Susceptible than WT Mice to EAE. Given the increased in vitro production of IL-17 and IFNγ by AV T cells and the acknowledged role of these cytokines as major pathologic mediators in EAE (21), we tested susceptibility of AVT mice to MOG-induced EAE. On immunization with $MOG_{35–55}$ peptide in complete Freund's adjuvant (CFA) (22), both groups of mice developed symptoms with roughly equivalent kinetics (Fig. 3*A* and Table S1); however, contrary to our expectations, AVT mice were consistently more resistant to the development of EAE than WT mice, with the difference in clinical scores becoming particularly significant late in the course of disease (Fig. 3*A* and Table S1). Analysis of spleen and lymph nodes at day 6 (when activated T cells begin to migrate into the CNS) (23) did not reveal any gross differences between WT and AVT cohorts: AVT mice still had lower numbers of Tregs and CD4 CD44^{hi}CD62L^{lo} activated/effector T cells in their spleens compared with WT, although these differences were not as apparent in lymph nodes (Fig. S6*A*). After brief (4 h) stimulation with PMA and ionomycin, the frequencies of IL-4–, IL-17–, and IFNγ-producing cells in the spleens of MOG-immunized AVT mice were diminished relative to WT (Fig. 3*B Left*); again, these differences were less apparent when lymph node cells were examined (Fig. 3*C Left*). In contrast, the frequency of IL-10–producing cells was significantly elevated in the lymph nodes of AVT mice compared with WT at day 6 as well as day 14 (Fig. 3 *B* and *C*).

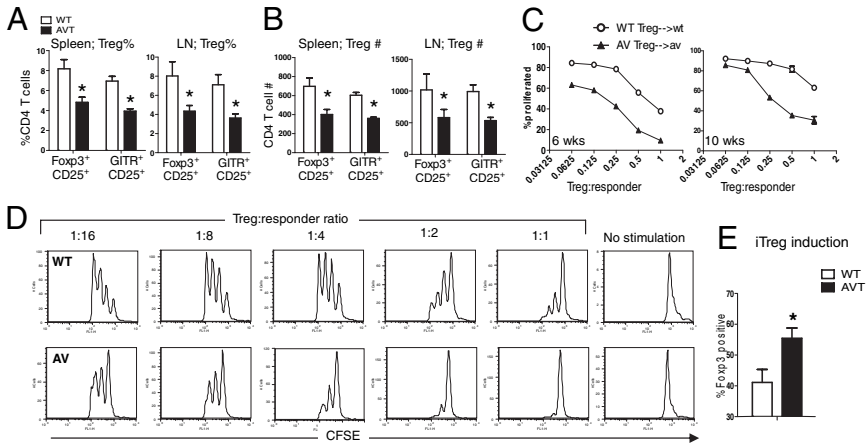

Fig. 2. Characteristics of natural and induced Tregs in AVT mice. Decreased frequency (*A*) and number (*B*) of Tregs in spleen and lymph nodes of AVT mice, relative to WT (age, 6 wks, $n = 4$ per group). (*C*) Increased suppressive effects of AV Tregs relative to WT Tregs on corresponding effectors; Tregs and effectors were isolated from 6- or 10-wk old mice (*Materials and Methods*). (*D*) Representative FACS profiles from the 6-wk time point. % proliferated, percentage of total cells having undergone one or more divisions, as measured by CFSE dilution. (*E*) Enhanced generation of iTregs from naive AV CD4 T cells relative to WT (*SI Materials and Methods*). $*P < 0.05$ by Student's t-test. Data are representative of at least two independent experiments.

Increased IL-10 Production by CD4 T Cells of AVT Mice. IL-10 is an immunomodulatory cytokine that is now known to be produced by all subsets of Th cells, including Th17 cells; its expression in Th1 and Th2 cells has been transcriptionally linked to NFAT1, and it has a documented ameliorative effect on the progression of EAE (24–26). Given the diminished EAE phenotype and increased numbers of IL-10–producing T cells in AVT mice (Fig. 3 and Table S1), we hypothesized that AV T cells might produce increased amounts of IL-10, as well as IL-17, in response to Th17 cues. This was indeed the case in vitro—on activation in the presence of TGFβ and IL-6, followed by restimulation with PMA/ionomycin, AV CD4 T cells yielded substantially higher frequencies of IL-10 producers and IL-10/IL-17 double producers compared with WT cells (Fig. 4*A*). As expected (27), the addition of IL-27 led to loss of the IL-17–producing population in both WT and AVT groups (Fig. 4*A Upper* and *Lower*; quantified in Fig. 4*B*).

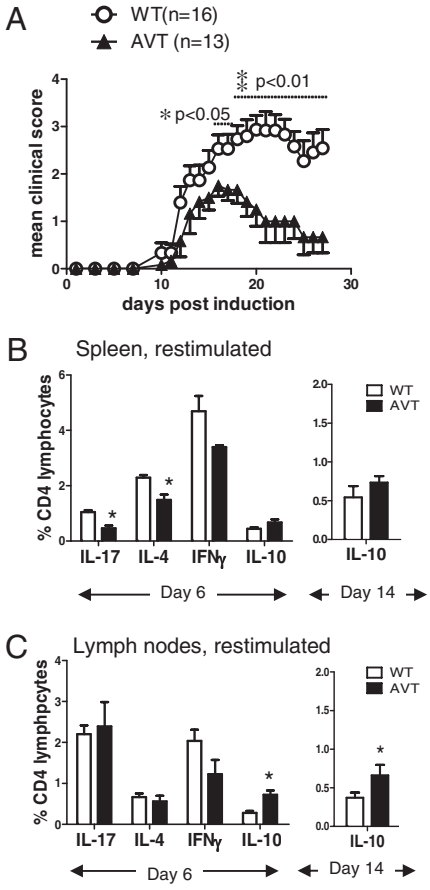

Fig. 3. Decreased susceptibility to EAE in AVT mice relative to WT littermates. (*A*) Representative experiment out of four independent trials; clinical scoring as described in *Materials and Methods*. $*P < 0.05$, $**P < 0.01$ by Student's *t*-test. (*B*, *C*) Cytokine production by CD4 T cells in *B*, spleen and *C*, lymph nodes at day 6 after MOG immunization. (*B* Right and *C* Right) Percentage of IL-10-producing CD4 T cells at day 14 after MOG immunization.

Increased Frequency of IL-10–Producing T Cells and Foxp3$^+$ Tregs in the CNS of AVT Mice During EAE. To ask if alterations in IL-10 production and Treg function noted in AV T cells in vitro might be responsible for reduced EAE-associated pathology in AVT mice in vivo, animals from both groups were killed at two time points after $MOG_{35–55}$ immunization: a relatively early time point after disease onset (day 14) and during established disease (day 20). At both time points, AVT mice had fewer cells in the CNS compared with WT mice (Fig. 5*A*), although they had more lymphocytes in spleen and lymph nodes (Fig. S6*B*). Despite the lower overall numbers of lymphocytes, AVT mice displayed a larger proportion of IL-10–producing cells in the CNS at days 14 and 20 (Fig. 5 *B* and *C*), although the IL-17/IL-10 double producers seen in vitro after Th17 differentiation (Fig. 4*A*) were not apparent in vivo. At the mRNA level, CD4 T cells derived from the CNS of AVT mice during established disease (at days 20 and 25 after immunization) had significantly higher amounts of IL-10 transcripts relative to WT and significantly lower amounts of the signature Th17 cytokines IL-17, IL-17F, and IL-21 (Fig. 5*D*). Notably, mRNA levels of the IL-23 receptor (IL-23Rα) and IFNγ were approximately 2-fold higher in AV CD4 T cells than in WT; the mRNA levels of IL-22, which plays a role in Th17-mediated skin inflammation rather than EAE, were similar in both groups of mice (Fig. 5*D*) (28).

At day 14, when WT and AVT mice show little difference in their EAE scores (Fig. 3*A* and Table S1), there was no difference in Treg frequencies within the CNS of both cohorts (Fig. 5*E*). However, by day 20, when EAE scores of the two groups have diverged significantly and AVT mice show faster recovery (Fig. 3*A* and Table S1), there were significantly higher percentages of CD4 Foxp3$^+$ Tregs in the CNS of AVT mice relative to controls (Fig. 5*F*). The lower lymphocyte numbers isolated from the CNS of AVT mice at day 20, relative to WT, could reflect active suppression by the higher proportion of Tregs within the CNS of AVT animals—we noted a significant reduction in levels of IL-2 transcripts in AV CD4 T cells compared with WT, suggesting a diminished T-cell proliferative response (Fig. 5*D*). Thus, there appear to be at least two powerful immunomodulatory mechanisms, increased IL-10 production and increased accumulation of Foxp3$^+$ Tregs in the CNS, that could account for the significantly milder EAE phenotype observed in AVT mice. AV Tregs could

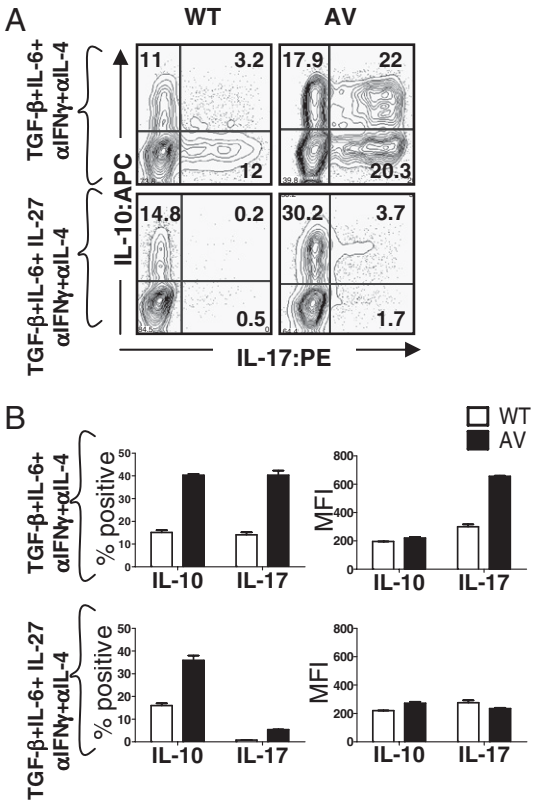

Fig. 4. Increased IL-10 production by CD4 T cells from AVT mice. (*A*) Naïve CD4 T cells were cultured under Th17 conditions in vitro and restimulated on day 4 with 20 nM PMA and 500 nM ionomycin (as in Fig. 1 *B* and *C*). Data depicted are representative of at least two independent experiments. (*B*) Graphical representation of the FACS data, $n = 2$ mice per group. (*Left*) Total percent of IL-17- and IL-10 positive cells. (*Right*) Mean fluorescence intensity (MFI) for each cytokine.

contribute to increased IL-10 production in the CNS as judged by analysis of $CD4^+$ $GITR^+$ T cells, which include Tregs as well as activated T cells (Fig. S6*D*).

Direct Binding of NFAT1 to *Il17/Il17f* and *Il10* Loci in Cells Undergoing Th17 Differentiation. The *Il17/Il17f* locus undergoes chromatin structural changes during Th17 differentiation—multiple conserved non-coding sequences (CNCS) become hyperacetylated at histone H3 in a Th17 lineage-specific manner and can, thus, be regarded as putative regulatory elements (29) (Fig. S7*C*). Of these, CNCS2a seems to be particularly important: it binds the orphan nuclear receptor RORγt and the AP-1 family transcription factor Batf, both essential for Th17 differentiation (30, 31). CNCS2a also enhances transactivation of the minimal *Il17* promoter by RORγt and RORα (30). Multiple NFAT sites are present in the evolutionarily conserved CNCS regions identified in the *Il17/Il17f* locus (Fig. S8*A*) (29). To test whether NFAT1 binds to *Il17/Il17f* CNCS regions in Th17 cells, ChIP was performed using naïve CD4 T cells differentiated under Th17-polarizing conditions. NFAT1 was found to bind specifically to a triad of CNCS regions, CNCS2a, CNCS3, and CNCS7, flanking the *Il17* and *Il17f* genes in WT (Fig. 6*A* and Fig. S7*C*) and AV T cells (Fig. S8*B*).

Relatively little is known about the regulation of IL-10 transcription during Th17 differentiation. Numerous *cis*-regulatory elements in the *Il10* locus have been mapped, and some have been shown to be important for transcriptional regulation of IL-10 production, mainly in Th2 cells (24, 32, 33). Of these, CNCS9, located 9 kb upstream of the transcription start site of the *Il10* gene, is a critical enhancer region (Fig. S7*D*) containing three NFAT1 binding sites—NFAT1 binds CNCS9 in Th2 cells to regulate IL-10 production in concert with IRF4 (24). We show here that NFAT1 also binds CNCS9 during Th17 differentiation in both WT and AV T cells (Fig. 6*B*).

Discussion

In this study, we asked how increasing signal strength in the Ca^{2+} arm of the TCR signaling pathway would influence T cell differentiation in vitro and T cell-mediated immune responses in vivo. We used transgenic mice expressing a hyperactivable form of NFAT1, AV-NFAT1, selectively within the T cell compartment. Given its increased affinity for calcineurin and reduced affinity for CK1, AV-NFAT1 constitutes a tunable version of NFAT1—it continues to respond to signaling cues but with lower activation thresholds, representing an in vivo correlate of strong TCR signals and as such, marks an improvement over CA-NFAT proteins used in previous studies (11). Expression of AV-NFAT1 from the R26 locus does not appreciably increase the total amount of NFAT1 in cells, perhaps because AV-NFAT1, like CA-NFAT proteins, is more susceptible than WT NFAT1 to feedback degradation in cells (10, 11). Thus, the observed effects can be attributed to increased signal responsiveness of hyperactivable NFAT1 rather than to a major increase in overall NFAT1 expression.

The balance of Th1/Th2 differentiation can be skewed by altering the strength of TCR ligation, stronger TCR signals driving Th1 responses and weak signals resulting in Th2 differentiation (34). The substantial Th1 bias displayed by CD4 AV T cells is in line both with the established link between heightened TCR signaling and Th1 differentiation and with the previously shown Th2 bias of $NFAT1^{-/-}$ T cells (14, 15). The impact of AV-NFAT1 on Treg development was complex. Relative to WT, AVT mice had lower steady-state levels of Tregs within their peripheral lymphoid organs, which could reflect the dual effect of increased TCR signaling on nTreg differentiation. Whereas strong TCR signals within the thymus are required for nTreg generation, Treg proportions are often decreased in response to increased levels of antigen, presumably because of negative selection of developing thymocytes by excessive signaling through the TCR (35). Functionally, however, AV Tregs showed increased suppressive capacity in vitro relative to WT Tregs, confirming the importance of NFAT in maintenance of the Treg suppressive program (7). Finally, more efficient iTreg generation in AVT mice is consistent with the involvement of NFAT in up-regulating Foxp3 expression (6, 8).

Whereas AV T cells showed a considerable increase in IL-17 production in vitro, AVT mice were more resistant than WT mice to the development of EAE. Several factors seem to be in play. First, despite the pronounced Th17 bias in vitro, AVT mice exhibited dampening of IL-17, IL-17F, and IL-21 production at a transcriptional level in response to MOG/CFA immunization. There did not appear to be an overall blunting of the Th17 program, because AV CD4 T cells had significantly higher amounts of IL-23R mRNA within the CNS compared with WT (3). Second, CD4 T cells from AVT mice produced substantially higher levels of IL-10 than WT, both in vitro and during MOG-induced EAE. Finally, AVT mice contained higher proportions of $Foxp3^+$ Tregs within their CNS during the later stages of disease, coinciding with a marked reduction in clinical scores compared with WT littermates. Late-phase EAE is associated with increased levels of TGFβ in the CNS (36)—the progressive increase in $Foxp3^+$ Tregs in the CNS of AVT mice could be attributable to enhanced TGFβ-mediated up-regulation of Foxp3 and iTreg generation; alternatively, the existing Treg pool in AVT mice might show increased proliferation or migration into the CNS. Already differentiated Th17 cells up-regulate IL-10 expression in response to continued exposure to TGFβ and IL-6 (25), which could account for the increased IL-10 production in AVT mice. Tregs and IL-10–producing cells both have well-documented, possibly overlapping, roles in the restriction of pathogenic responses and subsequent recovery from EAE (25, 37).

Although CD4 T cells from the CNS of AVT and WT mice contained equivalent levels of Foxp3 mRNA transcripts, AV CD4 T cells exhibited a marked decrease in levels of cyclic nucleotide phosphodiesterase 3B (PDE 3B) (Fig. S7*A*)—PDE3B down-

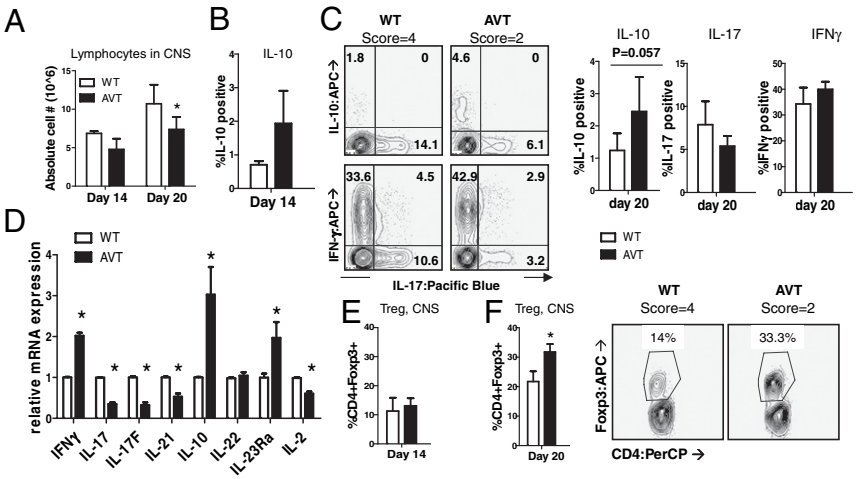

Fig. 5. Increased frequency of IL-10-producing T cells and Tregs in the CNS of AVT mice. (*A*) Absolute numbers of lymphocytes purified from CNS of AVT and WT mice following MOG immunization; at day 14: $n = 2$, score = 2 for both WT and AVT mice; at day 20: $n = 2$, score = 4 for WT and $n = 2$, score = 2 for AVT mice. CNS lymphocytes were stimulated with 20 nM PMA and 1μM ionomycin for 4 h, stained for FACS and gated on the CD4 positive population. (*B*) IL-10 production by CNS-resident CD4 T cells from WT and AVT mice at day 14. (*C*) IL-10, IL-17 and IFNγ production by CNS-resident CD4 T cells from WT and AVT mice at day 20; (*Left*) representative flow cytometry. (*D*) CD4 T cells were purified from CNS lymphocytes, total RNA was isolated, and mRNA expression was quantified by real-time RT-PCR (*Materials and Methods*). Data are representative of two independent experiments done with cells isolated at a late stage of disease (days 20 and 25 following MOG immunization); *$P \leq 0.05$ by Student's *t*-test. CD4 Foxp3$^+$ T cells were quantified by intracellular Foxp3 staining of CNS lymphocytes at (*E*), day 14 and (*F*), day 20. Representative flow cytometry shown in *Right*. The data depicted were obtained from two independent experiments.

regulation is a critical aspect of Foxp3-dependent maintenance of the Treg program (38). We did not observe significant differences between WT and AV CD4 T cells from the CNS comparing mRNA levels of a number of other genes associated with Tregs, anergy induction, or both (Fig. S7*A*). AV and WT CD4 T cells expressed equivalent mRNA levels of the C-C chemokine receptor 6 (CCR6) and its ligand CCL20, CCR6 being crucial for CNS entry of MOG-reactive T cells and subsequent development of EAE (23) (Fig. S7*B*); thus, there did not seem to be an overt trafficking defect involving this chemokine axis.

Interestingly, CD4 T cells isolated from the CNS of AVT mice during late-stage EAE had higher levels of IFNγ transcripts compared with WT controls. The role of IFNγ in EAE pathogenesis is somewhat equivocal—IFNγ is associated with a proinflammatory role and increased myelin damage during EAE (21), but mice deficient for IFNγ or its receptor remain susceptible to EAE, actually developing a more aggressive form of the disease (39). More recently, increased intrathecal levels of IFNγ have been ascribed a protective function in EAE through activation of the integrated stress response in myelin oligodendrocytes, which increases their resistance to cytotoxic cell death and decelerates inflammation-induced demyelination/axonal damage (39).

In summary, we show that NFAT1 plays a direct role in transcriptional up-regulation of both IL-17 and IL-10 in T cells undergoing Th17 differentiation. NFAT1 occupies three CNCS regions in the *Il17/Il17f* locus in stimulated Th17 cells: upstream of *Il17* at CNCS2a, upstream of *Il17f* at CNCS7, and in the intergenic region at CNCS3. In addition, NFAT1 binds to the critical CNCS9-enhancer element in the *Il10* locus in Th17 cells. On Th17 differentiation in vitro, proinflammatory IL-17 and immunosuppressive IL-10 are simultaneously up-regulated in AV CD4 T cells to a far greater extent than in WT T cells. In vivo, in response to MOG/CFA-derived cues, the net balance in AVT mice is tipped towards reduced expression of Th17 cytokines and increased production of IL-10 and Tregs, resulting in a significantly milder EAE phenotype. Although surprising, this outcome is consistent with previous observations that decreased NFAT function can be associated with dramatic lymphoproliferative disease, as observed in mice lacking NFAT1 and NFAT4 on the one hand (40), or lacking store-operated Ca^{2+} entry and therefore, signaling through the Ca^{2+}/NFAT pathway on the other [human patients lacking expression of the Ca^{2+} sensor STIM1 (41); mice lacking STIM1 and STIM2 expression in T cells (42, 43)]. NFAT1, thus, acts as a gatekeeper for multiple divergent pathways downstream of T-cell activation (Th1/Th2/Th17/Treg)—the AVT trangenics illustrate its role as a calibrator for graded TCR signals, excessive activation resulting in immunomodulation rather than exacerbation of autoimmunity. Regardless of mechanism, our results indicate that augmentation of NFAT-dependent transcription might be therapeutic in at least some cases of autoimmune disease and may explain the limited efficacy of CsA and other calcineurin inhibitors in autoimmunity in the clinic (44).

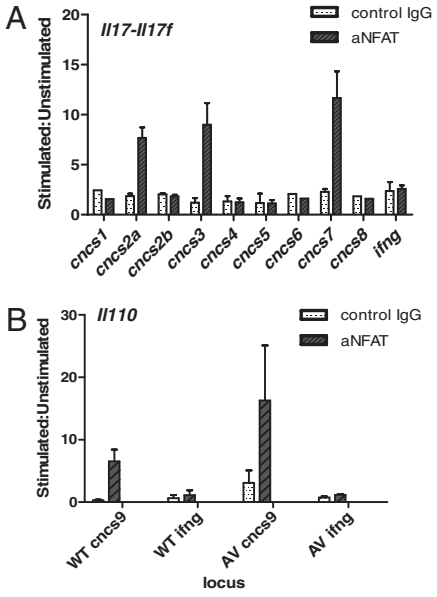

Fig. 6. NFAT1 binds the *Il17/Il17f* and *Il-10* loci in CD4 T cells undergoing Th17 differentiation. (*A*) NFAT1 binds *CNCS2a, CNCS3* and *CNCS7* in the *Il17/Il17f* locus and (*B*) *CNCS9* in the *Il10* locus in Th17 differentiated cells. IFNγ is used as a negative control locus that is not accessible in cells undergoing Th17 differentiation (29). Data are representative of at least two independent experiments.

Materials and Methods

Mice. Generation of transgenic R26$^{AV\text{-}NFAT1}$/R26$^+$ and R26$^{AV\text{-}NFAT1}$/R26$^{AV\text{-}NFAT1}$ animals has been described previously (10). CD4-Cre mice were purchased from Taconic. All mice were on a C57BL/6 background and housed under pathogen-free conditions in the animal facility at the Immune Disease Institute (IDI), Harvard Medical School. All experiments were performed in accordance with protocols approved by the Harvard University Institutional Animal Care and Use Committee and IDI.

In Vitro T-Cell Differentiation. CD4 T cells were isolated from spleens and lymph nodes of mice using the Dynal CD4 T-cell positive-isolation kit (Invitrogen) and activated with αCD3+αCD28 for 48 h under nonpolarizing (Th0), Th1, or Th2 conditions (*SI Materials and Methods*). CD4CD25$^+$ T cells were depleted from purified CD4 T cells using a CD25 microbead MACS kit (Mil-

IMMUNOLOGY

tenyi Biotech), and CD4CD25$^-$ T cells were activated with αCD3+αCD28 under iTreg- or Th17-inducing conditions (*SI Materials and Methods*).

Treg Suppression Assay. Carboxyfluorescein succinimidyl ester (CFSE)-labeled CD4 CD25$^-$ responder T cells were incubated with CD4 CD25$^+$ Tregs and mitomycin C-treated splenocytes in the presence of 0.3 μg/mL αCD3. Cells were fixed using a fixation/permeabilization solution (eBioscience) to quench EGFP fluorescence in AV responder T cells; CFSE dilution was measured by FACS 72 h postactivation.

EAE Induction. $MOG_{35–55}$ peptide was synthesized at the Tufts University Core Facility; 8- to 10-wk-old female mice were immunized with $MOG_{35–55}$ emulsified in CFA as described previously (22). Briefly, lyophilized $MOG_{35–55}$ was reconstituted in PBS and mixed 1:1 with CFA [5 mg/mL *Mycobaterium tuberculosis* (H37Ra; BD Pharmingen) in incomplete Freund's adjuvant (Sigma)]. Each mouse was s.c. immunized with 100 μg of MOG peptide and an i.p. injection of 200 ng of Pertussis toxin (Calbiochem). Mice were monitored daily and scored for disease based on the following clinical scale: 0, healthy; 1, flaccid tail; 2, ataxia/paresis of hind limbs; 3, paralysis of hind limbs; 4, tetraparalysis; 5, moribund or death.

Isolation of CNS Lymphocytes. Brains and spinal cords were harvested from euthanized mice after perfusion with cold PBS. CNS tissue was minced and digested using a mixture of Liberase C1 and DNase I (Roche) for ~30 min at 37 °C. Homogenized tissue was passed through 70-μm filters and fractionated by density-gradient centrifugation using a combination of 30–70% Percoll (Sigma-Aldrich). Mononuclear cells were obtained by collecting buffy coats from the liquid interface. Cells were stimulated for intracellular cytokine FACS. CD4 T cells were isolated from CNS lymphocytes using the Dynal CD4 positive-selection kit (Invitrogen).

Real-Time RT-PCR. RNA was isolated from cell pellets using the RNeasy kit (Qiagen) followed by first-strand synthesis using SuperScript III (Invitrogen). Synthesized cDNA was amplified using the FastStart Universal SYBR Green Master Mix (Roche), and PCR data was collected using the StepOnePlus Real-Time PCR System (Applied Biosystems). Gene expression was normalized to an endogenous GAPDH control using the $\Delta\Delta C_T$ method; primer sequences are listed in Table S2.

ChIP. ChIP was performed on lysates from Th17-differentiated cells (*SI Materials and Methods*), using rabbit polyclonal αNFAT1 (67.1) or polyclonal rabbit antiserum (control) followed by the addition of protein A beads. Beads were washed and treated with RNase A and Proteinase K. After cross-link reversal by incubation at 65 °C, DNA was isolated from the mixture using QIAquick spin columns (Qiagen) and used as a template for real-time PCR. Primers used for ChIP PCRs have been described elsewhere (24, 29).

Statistical Analysis. Results have been depicted as mean ± SEM or mean ± range. The unpaired Student *t* test was used to assess differences between analyzed groups. Differences in FACS staining data between groups from one experiment to the other were analyzed using the paired *t* test. Values of $P < 0.05$ were considered significant.

ACKNOWLEDGMENTS. We thank Edward D. Lamperti and Curtis Gelinas for help with mouse colony maintenance and genotyping. This study was supported by T32 Training Grant 5T32AI070085-03 (to S.G.), a Deutsche Krebshilfe Postdoctoral Fellowship (to M.R.M.), an Irvington Institute Fellowship of the Cancer Research Institute (to M.R.M.), National Institutes of Health Grant CA42471 (to A.R.), and Juvenile Diabetes Research Foundation Grants 16-2007-427 and 17-2010-421 (to A.R.).

1. Hogan PG, Chen L, Nardone J, Rao A (2003) Transcriptional regulation by calcium, calcineurin, and NFAT. *Genes Dev* 17:2205–2232.
2. Zhou L, Chong MM, Littman DR (2009) Plasticity of CD4+ T-cell lineage differentiation. *Immunity* 30:646–655.
3. Dong C (2008) TH17 cells in development: An updated view of their molecular identity and genetic programming. *Nat Rev Immunol* 8:337–348.
4. Spolski R, Leonard WJ (2008) Interleukin-21: Basic biology and implications for cancer and autoimmunity. *Annu Rev Immunol* 26:57–79.
5. Gomez-Rodriguez J, et al. (2009) Differential expression of interleukin-17A and -17F is coupled to T cell receptor signaling via inducible T cell kinase. *Immunity* 31:587–597.
6. Zheng Y, et al. (2010) Role of conserved non-coding DNA elements in the Foxp3 gene in regulatory T-cell fate. *Nature* 463:808–812.
7. Wu Y, et al. (2006) FOXP3 controls regulatory T cell function through cooperation with NFAT. *Cell* 126:375–387.
8. Tone Y, et al. (2008) Smad3 and NFAT cooperate to induce Foxp3 expression through its enhancer. *Nat Immunol* 9:194–202.
9. Gwack Y, et al. (2006) A genome-wide Drosophila RNAi screen identifies DYRK-family kinases as regulators of NFAT. *Nature* 441:646–650.
10. Müller MR, et al. (2009) Requirement for balanced Ca/NFAT signaling in hematopoietic and embryonic development. *Proc Natl Acad Sci USA* 106:7034–7039.
11. Macián F, et al. (2002) Transcriptional mechanisms underlying lymphocyte tolerance. *Cell* 109:719–731.
12. Aramburu J, et al. (1999) Affinity-driven peptide selection of an NFAT inhibitor more selective than cyclosporin A. *Science* 285:2129–2133.
13. Okamura H, et al. (2004) A conserved docking motif for CK1 binding controls the nuclear localization of NFAT1. *Mol Cell Biol* 24:4184–4195.
14. Kiani A, Viola JP, Lichtman AH, Rao A (1997) Down-regulation of IL-4 gene transcription and control of Th2 cell differentiation by a mechanism involving NFAT1. *Immunity* 7:849–860.
15. Rengarajan J, Tang B, Glimcher LH (2002) NFATc2 and NFATc3 regulate T(H)2 differentiation and modulate TCR-responsiveness of naïve T(H)cells. *Nat Immunol* 3: 48–54.
16. Teixeira LK, et al. (2005) IFN-gamma production by CD8+ T cells depends on NFAT1 transcription factor and regulates Th differentiation. *J Immunol* 175:5931–5939.
17. Chen Z, Laurence A, O'Shea JJ (2007) Signal transduction pathways and transcriptional regulation in the control of Th17 differentiation. *Semin Immunol* 19:400–408.
18. Zhou L, et al. (2008) TGF-beta-induced Foxp3 inhibits T(H)17 cell differentiation by antagonizing RORgammat function. *Nature* 453:236–240.
19. Huber M, et al. (2008) IRF4 is essential for IL-21-mediated induction, amplification, and stabilization of the Th17 phenotype. *Proc Natl Acad Sci USA* 105:20846–20851.
20. Korn T, et al. (2007) IL-21 initiates an alternative pathway to induce proinflammatory T(H)17 cells. *Nature* 448:484–487.
21. Korn T, Bettelli E, Oukka M, Kuchroo VK (2009) IL-17 and Th17 cells. *Annu Rev Immunol* 27:485–517.
22. Veldhoen M, Hocking RJ, Flavell RA, Stockinger B (2006) Signals mediated by transforming growth factor-beta initiate autoimmune encephalomyelitis, but chronic inflammation is needed to sustain disease. *Nat Immunol* 7:1151–1156.
23. Reboldi A, et al. (2009) C-C chemokine receptor 6-regulated entry of TH-17 cells into the CNS through the choroid plexus is required for the initiation of EAE. *Nat Immunol* 10:514–523.
24. Lee CG, et al. (2009) A distal cis-regulatory element, CNS-9, controls NFAT1 and IRF4-mediated IL-10 gene activation in T helper cells. *Mol Immunol* 46:613–621.
25. McGeachy MJ, et al. (2007) TGF-beta and IL-6 drive the production of IL-17 and IL-10 by T cells and restrain T(H)-17 cell-mediated pathology. *Nat Immunol* 8:1390–1397.
26. Maynard CL, Weaver CT (2008) Diversity in the contribution of interleukin-10 to T-cell-mediated immune regulation. *Immunol Rev* 226:219–233.
27. Stumhofer JS, et al. (2007) Interleukins 27 and 6 induce STAT3-mediated T cell production of interleukin 10. *Nat Immunol* 8:1363–1371.
28. Eyerich S, et al. (2009) Th22 cells represent a distinct human T cell subset involved in epidermal immunity and remodeling. *J Clin Invest* 119:3573–3585.
29. Akimzhanov AM, Yang XO, Dong C (2007) Chromatin remodeling of interleukin-17 (IL-17)-IL-17F cytokine gene locus during inflammatory helper T cell differentiation. *J Biol Chem* 282:5969–5972.
30. Yang XO, et al. (2008) T helper 17 lineage differentiation is programmed by orphan nuclear receptors ROR alpha and ROR gamma. *Immunity* 28:29–39.
31. Schraml BU, et al. (2009) The AP-1 transcription factor Batf controls T(H)17 differentiation. *Nature* 460:405–409.
32. Im SH, Hueber A, Monticelli S, Kang KH, Rao A (2004) Chromatin-level regulation of the IL10 gene in T cells. *J Biol Chem* 279:46818–46825.
33. Jones EA, Flavell RA (2005) Distal enhancer elements transcribe intergenic RNA in the IL-10 family gene cluster. *J Immunol* 175:7437–7446.
34. Constant SL, Bottomly K (1997) Induction of Th1 and Th2 CD4+ T cell responses: The alternative approaches. *Annu Rev Immunol* 15:297–322.
35. Sakaguchi S, Yamaguchi T, Nomura T, Ono M (2008) Regulatory T cells and immune tolerance. *Cell* 133:775–787.
36. Chen Y, Hancock WW, Marks R, Gonnella P, Weiner HL (1998) Mechanisms of recovery from experimental autoimmune encephalomyelitis: T cell deletion and immune deviation in myelin basic protein T cell receptor transgenic mice. *J Neuroimmunol* 82: 149–159.
37. Korn T, et al. (2008) IL-6 controls Th17 immunity in vivo by inhibiting the conversion of conventional T cells into Foxp3+ regulatory T cells. *Proc Natl Acad Sci USA* 105: 18460–18465.
38. Gavin MA, et al. (2007) Foxp3-dependent programme of regulatory T-cell differentiation. *Nature* 445:771–775.
39. Lin W, et al. (2007) The integrated stress response prevents demyelination by protecting oligodendrocytes against immune-mediated damage. *J Clin Invest* 117: 448–456.
40. Ranger AM, Oukka M, Rengarajan J, Glimcher LH (1998) Inhibitory function of two NFAT family members in lymphoid homeostasis and Th2 development. *Immunity* 9: 627–635.
41. Picard C, et al. (2009) STIM1 mutation associated with a syndrome of immunodeficiency and autoimmunity. *N Engl J Med* 360:1971–1980.
42. Oh-Hora M, et al. (2008) Dual functions for the endoplasmic reticulum calcium sensors STIM1 and STIM2 in T cell activation and tolerance. *Nat Immunol* 9:432–443.
43. Oh-hora M, Rao A (2009) The calcium/NFAT pathway: Role in development and function of regulatory T cells. *Microbes Infect* 11:612–619.
44. Steck AJ, Regli F, Ochsner F, Gauthier G (1990) Cyclosporine versus azathioprine in the treatment of multiple sclerosis: 12-month clinical and immunological evaluation. *Eur Neurol* 30:224–228.